Inorganic Chemistry

Article

La₂U₂Se₉: An Ordered Lanthanide/Actinide Chalcogenide with a Novel Structure Type

Daniel E. Bugaris,[†] Roy Copping,[‡] Tolek Tyliszczak,[§] David K. Shuh,[‡] and James A. Ibers*,[†]

[†]*Department of Chemistry, Northwestern University, Evanston, Illinois 60208-3113,* [‡]*Chemical Sciences Division, and* [§]*Advanced Light Source, Lawrence Berkeley National Laboratory, Berkeley, California 94720*

The compound La₂U₂Se₉ was obtained in high yield from the stoichiometric reaction of the elements in an Sb₂Se₃ flux at 1123 K. The compound, which crystallizes in a new structure type in space group *Pmma* of the orthorhombic system, has a three-dimensional structure with alternating U/Se and La/Se layers attached via three independent, infinite polyselenide chains. The U atom has a monocapped square antiprismatic coordination of Se atoms, whereas one La atom is bicapped square prismatic and the other La atom is trigonal prismatic. La₂U₂Se₉ displays an antiferromagnetic transition at T_N = 5 K; above 50 K, the paramagnetic behavior can be fit to the Curie−Weiss law, yielding a μ_{eff} of 3.10(1) μ_B/U. The low-temperature specific heat of La₂U₂Se₉ exhibits no anomalous behavior near the Néel temperature that might indicate long-range magnetic ordering or a phase transition. X-ray absorption near-edge structure (XANES) spectra have confirmed the assignment of formal oxidation states of +III for lanthanum and +IV for uranium in La₂U₂Se₉.

Introduction

The necessity of separating An³⁺ species from Ln³⁺ species (An = actinide; Ln = lanthanide) in the nuclear fuel cycle has prompted significant solution chemistry in which the structural relationships between the lanthanides and the actinides have been examined.[1] To assess the differences in chemical bonding, analogous An and Ln compounds have been synthesized and characterized in the solid state. However, comparatively little work has been carried out on mixed lanthanide/actinide solid-state systems.

The vast majority of extended solid-state structures incorporating both a lanthanide and an early actinide that have been characterized either exhibit Ln/An disorder or are ordered variants of known actinide or lanthanide binary compounds. Disorder is the rule because the ionic radii of Ln³⁺ and An³⁺, and to a lesser extent An⁴⁺, are very similar (Figure 1). Disordered examples, such as (Ln,Th)O₂ (Ln = La, Nd, Sm, Gd),[2] (Ln,U)N (Ln = La−Nd, Sm, Gd, Dy, Er),[3] (Ln,U)₃Q₄ (Ln = La, Ce, Pr; Q = S, Se, Te),[4] (Ln,U)S (Ln = Pr, Nd),[5] and (Ln,U)Te₃ (Ln ≠ Pm, Eu),[6,7] feature Ln and An atoms occupying the same crystallographic site, thus obscuring any differences in their bonding. There are also instances where the lanthanide substitutes in a particular position in an actinide binary to yield an ordered variant, or vice versa. For example, the U₃S₅ structure type,[8] with two crystallographically unique U sites, can be rationalized as (U³⁺)₂(U⁴⁺)(S²⁻)₅. Analogues of this structure type have been prepared where the Ln³⁺ preferentially substitutes on the U³⁺ site to give Ln₂UQ₅ (Ln = La−Sm; Q = S, Se).[9,10] Similarly, the Tb₇O₁₂ structure type,[11] with two crystallographically unique Tb sites, can be substituted with Ln and U to give (Ln³⁺)₆(U⁶⁺)O₁₂ (Ln = La, Lu).[12,13] These ordered variants provide some insight into the bonding differences between Ln and An. However, a novel structure type would provide a more useful comparison.

Although not derived from a binary compound, Yb₁₀.₈U₃.₇S₂₂[14] is in fact isostructural with the known

*To whom correspondence should be addressed. E-mail: ibers@chem.northwestern.edu.

(1) Nash, K. L.; Madic, C.; Mathur, J. N.; Lacquement, J. In *The Chemistry of the Actinide and Transactinide Elements*, 3rd ed.; Morss, L. R., Edelstein, N. M., Fuger, J., Eds.; Springer: Dordrecht, The Netherlands, 2006; Vol. *4*, pp 2622−2798.

(2) Brauer, G.; Gradinger, H. *Z. Anorg. Allg. Chem.* **1954**, *276*, 209–226.

(3) Ettmayer, P.; Waldhart, J.; Vendl, A. *Monatsh. Chem.* **1979**, *110*, 1109–1112.

(4) Demoncy, P.; Khodadad, P. *Ann. Chim. (Paris)* **1970**, *5*, 341–356.

(5) Troc, R. *Physica B+C* **1980**, *102*, 233–236.

(6) Slovyanskikh, V. K.; Kuznetsov, N. T. *Russ. J. Inorg. Chem. (Transl. of Zh. Neorg. Khim.)* **1990**, *35*, 447.

(7) Slovyanskikh, V. K.; Kuznetsov, N. T.; Gracheva, N. V.; Kipiani, V. G. *Russ. J. Inorg. Chem. (Transl. of Zh. Neorg. Khim.)* **1985**, *30*, 1720–1721.

(8) Potel, M.; Brochu, R.; Padiou, J.; Grandjean, D. *C. R. Seances Acad. Sci., Ser. C* **1972**, *275*, 1419–1421.

(9) Noël, H.; Prigent, J. *Physica B+C* **1980**, *102*, 372–379.

(10) Slovyanskikh, V. K.; Kuznetsov, N. T.; Gracheva, N. V. *Russ. J. Inorg. Chem. (Transl. of Zh. Neorg. Khim.)* **1984**, *29*, 960–961.

(11) Baenziger, N. C.; Eick, H. A.; Schuldt, H. S.; Eyring, L. *J. Am. Chem. Soc.* **1961**, *83*, 2219–2223.

(12) Hinatsu, Y.; Masaki, N.; Fujino, T. *J. Solid State Chem.* **1988**, *73*, 567–571.

(13) Bartram, S. F. *Inorg. Chem.* **1966**, *5*, 749–754.

(14) Rodier, N.; Tien, V. *Bull. Soc. Fr. Mineral. Cristallogr.* **1976**, *99*, 8–12.
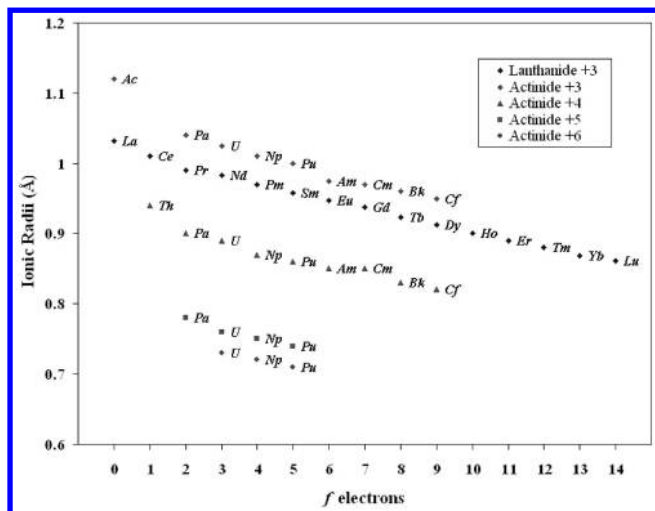
Figure 1. Ionic radii (Å) versus number of f electrons for the Ln^{3+} and the An^{n+} ($n = 3-6$) cations.[29]

interlanthanide $Lu_{11}Ce_4S_{22}$.[15] To achieve charge balance for this compound, the authors have suggested both mixed oxidation states for U (+III and +IV) and Yb (+II and +III), as well as fractional occupation of four of the eight crystallographic sites occupied by the metals. These anomalies may indicate possible disorder between U and Yb, as was observed in $Ln_2UO_2S_3$ (Ln = Yb, Y).[16]

To the best of our knowledge, there are no new structure types (not derived from a binary or a "pseudo-binary" interlanthanide compound) in the literature where Th and Ln occupy unique crystallographic sites, and only six where U and Ln do: $Cs_{11}Eu_4(UO_2)_2(P_2O_7)_6(PO_4)$,[17] $Nd[(UO_2)_3O$-$(OH)(PO_4)_2]\cdot6H_2O$,[18] $H_2[Nd_2(H_2O)_{12}UMo_{12}O_{42}]\cdot12H_2O$,[19] $(NH_4)_2(Er_2UMo_{12}O_{42})(H_2O)_{22}$,[20] $Ln_3UO_6Cl_3$ (Ln = La, Pr, Nd),[21] and $EuUI_6$.[22] Np is the only other actinide to form a new structure type with Ln, in the compound $La(NpO_2)_3$-$(NO_3)_6\cdot nH_2O$.[23] In these seven compounds the Ln and An atoms are surrounded by hard ligands, whereas softer ligands, such as N, S, and Se, have proven to be more effective for the separation of lanthanides from actinides.[1] We report here the synthesis, structure, and characterization of $La_2U_2Se_9$, the first ordered lanthanide/actinide chalcogenide with a novel structure type.

Experimental Section

Synthesis. The following reagents were used as obtained: U turnings (depleted, Oak Ridge National Laboratory), La (Cerac, 99.9%), Se (Cerac, 99.999%), filings from Ba rod

(Johnson Matthey, 99.5%), Sb (Aldrich, 99.5%), and Sb_2Se_3 (Alfa, 99%). Finely divided U powder was prepared by a modification[24] of the literature procedure.[25] The remaining reactants were used as obtained. Reactions were carried out in fused-silica tubes. The tubes were charged with reaction mixtures under an Ar atmosphere in a glovebox and then they were evacuated to ~10^{-4} Torr and flame-sealed. Selected single crystals from each reaction were examined with an energy-dispersive X-ray (EDX)-equipped Hitachi S-3400 scanning electron microscope.

The reaction mixture consisted of 0.13 mmol of U, 0.13 mmol of La, 0.13 mmol of Ba, 0.13 mmol of Sb, and 0.76 mmol of Se. The reaction mixture was placed in a computer-controlled furnace where it was heated to 1123 K in 17 h, kept at 1123 K for 6 days, cooled to 673 K in 150 h, annealed at 673 K for 7 days, and then the furnace was turned off. The product consisted of a few black metallic blocks of $La_2U_2Se_9$ in about 5% yield (based on U) and an amorphous black melt. EDX analysis of selected crystals showed the presence of La, U, and Se, but not of Ba or Sb. Although the black metallic sheen of the crystals dulls to a bronze upon extended exposure to ambient conditions there is no evidence of structural decomposition.

A crystal from this synthetic procedure was utilized for the collection of single-crystal X-ray diffraction data and subsequent structure determination. A rational synthesis was devised to yield sufficient material for physical property measurements. Here, the reaction mixture comprised a stoichiometric combination of the elements: 0.13 mmol of U, 0.13 mmol of La, and 0.59 mmol of Se, together with 0.21 mmol of Sb_2Se_3 added as flux. The heating profile was the same as that described above. The product consisted of a near quantitative yield of black metallic blocks of $La_2U_2Se_9$, as well as a few black prisms of La_2USe_5,[10] both of which could be manually separated from the shiny black columns of Sb_2Se_3.

Structure Determination. Single-crystal X-ray diffraction data were collected with the use of graphite-monochromatized MoKα radiation ($\lambda = 0.71073$ Å) at 100 K on a Bruker SMART-1000 CCD diffractometer.[26] The crystal-to-detector distance was 5.023 cm. Crystal decay was monitored by recollecting 50 initial frames at the end of the data collection. Data were collected by a scan of 0.3° in ω in groups of 606 frames at φ settings of 0°, 90°, 180°, and 270°. The exposure time was 20 s frame^{-1}. The collection of intensity data was carried out with the program SMART.[26] Cell refinement and data reduction were carried out with the use of the program SAINT v7.23a in APEX2.[27] Face-indexed absorption corrections were performed numerically with the use of the program SADABS.[26] The program SADABS was also employed to make incident beam and decay corrections.

The structure was solved with the direct-methods program SHELXS and refined with the full-matrix least-squares program SHELXL.[28] The identities of the metal (M) sites were assigned on the basis of M−Se distances. The nine-coordinate site exhibits M−Se distances less than 3.0 Å, which is appropriate for U^{4+} (ionic radius 1.19 Å) as opposed to La^{3+} (ionic radius 1.356 Å).[29] The final refinement included anisotropic displacement parameters and a secondary extinction correction. The program

(15) Rodier, N.; Tien, V. *Bull. Soc. Fr. Mineral. Cristallogr.* **1975**, *98*, 30–35.

(16) Jin, G. B.; Choi, E. S.; Ibers, J. A. *Inorg. Chem.* **2009**, *48*, 8227–8232.

(17) Pobedina, A. B.; Ilyukhin, A. B. *Russ. J. Inorg. Chem.* (*Transl. of Zh. Neorg. Khim.*) **1997**, *42*, 1006–1010.

(18) Piret, P.; Deliens, M.; Piret-Meunier, J. *Bull. Soc. Fr. Mineral. Cristallogr.* **1988**, *111*, 443–449.

(19) Samokhvalova, E. P.; Molchanov, V. N.; Tat'yanina, I. V.; Torchenkova, E. A. *Sov. J. Coord. Chem.* (*Engl. Transl.*) **1990**, *16*, 683–687.

(20) Tat'yanina, I. V.; Fomicheva, E. B.; Molchanov, V. N.; Zavodnik, V. E.; Bel'skii, V. K.; Torchenkova, E. A. *Sov. Phys. Crystallogr.* (*Engl. Transl.*) **1982**, *27*, 142–145.

(21) Henche, G.; Fiedler, K.; Gruehn, R. *Z. Anorg. Allg. Chem.* **1993**, *619*, 77–87.

(22) Beck, H. P.; Kühn, F. *Z. Anorg. Allg. Chem.* **1995**, *621*, 1659–1662.

(23) Grigor'ev, M. S.; Charushnikova, I. A.; Krot, N. N. *Radiochemistry* (*Transl. of Radiokhimiya*) **2005**, *47*, 549–551.

(24) Bugaris, D. E.; Ibers, J. A. *J. Solid State Chem.* **2008**, *181*, 3189–3193.

(25) Haneveld, A. J. K.; Jellinek, F. *J. Less-Common Met.* **1969**, *18*, 123–129.

(26) *SMART Version 5.054 Data Collection and SAINT-Plus Version 6.45a Data Processing Software for the SMART System*; Bruker Analytical X-Ray Instruments, Inc.: Madison, WI, 2003.

(27) *APEX2 Version 2009.5-1 and SAINT Version 7.34a Data Collection and Processing Software*; Bruker Analytical X-Ray Instruments, Inc.: Madison, WI, 2009.

(28) Sheldrick, G. M. *Acta Crystallogr., Sect. A: Found. Crystallogr.* **2008**, *64*, 112–122.

(29) Shannon, R. D. *Acta Crystallogr., Sect. A: Cryst. Phys. Diffr. Theor. Gen. Crystallogr.* **1976**, *32*, 751–767.

STRUCTURE TIDY[30] was employed to standardize the atomic coordinates. After refinement of this model for $La_2U_2Se_9$, the site occupancies of the three metal positions were allowed to vary. The resultant formula was $La_{2.06(3)}U_{1.94(3)}Se_9$. The values of $R(F)$ and $R_w(F_o^2)$ decreased from 0.0264 and 0.0741 to 0.0255 and 0.0709, respectively. These improvements were deemed to be inconsequential, given the uncertainties inherent in the determination of composition from X-ray diffraction data.[31] Additional crystallographic details are given in Table 1 and the Supporting Information. Selected metrical details are presented in Table 2.

Magnetic Susceptibility Measurements. Magnetic susceptibility as a function of temperature was measured on a 26.25 mg sample of ground single crystals of $La_2U_2Se_9$ with the use of a Quantum Design MPMS5 SQUID magnetometer. The sample was loaded into a gelatin capsule. Both zero-field cooled (ZFC) and field-cooled (FC) susceptibility data were collected between 2 and 300 K at an applied field of 500 G. All data were corrected for electron−core diamagnetism.[32]

Specific Heat Measurement. The specific heat C_p of $La_2U_2Se_9$ was measured in the temperature region 1.8 to 20 K with the use of a Quantum Design Physical Properties Measurement System (PPMS). A 6.0 mg quantity of single crystals was mounted with grease on the base of a heat-capacity puck. Similar measurements of the base and grease without the sample provided the background correction.

Scanning Transmission X-ray Microscopy (STXM) Spectromicroscopy. STXM spectromicroscopy at the Advanced Light Source-Molecular Environmental Sciences (ALS-MES) Beamline 11.0.2 was utilized to record images, elemental maps, and X-ray absorption near-edge structure (XANES) spectra at the La $3d_{5/2,3/2}$-edges ($M_{5,4}$), the U $4d_{5/2,3/2}$-edges ($N_{5,4}$), and Se $2p_{3/2,1/2}$-edges ($L_{3,2}$) from $La_2U_2Se_9$ to obtain element-specific oxidation state information.[33−36] The radioactive samples were powdered and sealed between two thin (100 nm) silicon nitride windows with epoxy before transfer to the He-purged STXM instrument. The spatial resolution for the La and U images and spectra was 40 nm, whereas for Se spectromicroscopy this was 50 nm. The errors in peak energy assignments are 0.04 eV for La and U spectra, and 0.13 eV for the Se spectra (refer to the Supporting Information for additional experimental details). The ALS-MES STXM data collection has been previously described in detail; spectra were extracted from image stacks (a complete set of registered images collected sequentially at each photon energy of a spectral scan).[37] All spectra were normalized to the incoming flux by integrating over the response from areas without sample particulates. Linear backgrounds were subtracted from most spectra; they were then smoothed and renormalized. The ALS operated at 500 mA of continuously stored electron beam during the data collection. The following compounds used as reference

(30) Gelato, L. M.; Parthé, E. *J. Appl. Crystallogr.* **1987**, *20*, 139–143.

(31) Mironov, Y. V.; Cody, J. A.; Albrecht-Schmitt, T. E.; Ibers, J. A. *J. Am. Chem. Soc.* **1997**, *119*, 493–498.

(32) *Theory and Applications of Molecular Diamagnetism*; Mulay, L. N., Boudreaux, E. A., Eds.; Wiley-Interscience: New York, 1976.
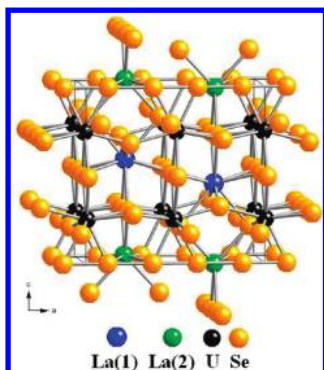
(33) Bluhm, H.; Andersson, K.; Araki, T.; Benzerara, K.; Brown, G. E.; Dynes, J. J.; Ghosal, S.; Gilles, M. K.; Hansen, H.-C.; Hemminger, J. C.; Hitchcock, A. P.; Ketteler, G.; Kilcoyne, A. L. D.; Kneedler, E.; Lawrence, J. R.; Leppard, G. G.; Majzlam, J.; Mun, B. S.; Myneni, S. C. B.; Nilsson, A.; Ogasawara, H.; Ogletree, D. F.; Pecher, K.; Salmeron, M.; Shuh, D. K.; Tonner, B.; Tyliszczak, T.; Warwick, T.; Yoon, T. H. *J. Electron Spectrosc. Relat. Phenom.* **2006**, *150*, 86–104.

(34) Janousch, M.; Copping, R.; Tyliszczak, T.; Castro-Rodriguez, I.; Shuh, D. K. *Mater. Res. Soc. Symp. Proc.* **2008**, *1104*, 165–170.
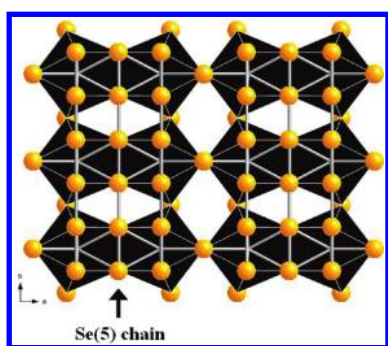
(35) Minasian, S. G.; Krinsky, J. L.; Rinehart, J. D.; Copping, R.; Tyliszczak, T.; Janousch, M.; Shuh, D. K.; Arnold, J. *J. Am. Chem. Soc.* **2009**, *131*, 13767–13783.

(36) Stöhr, J. *NEXAFS Spectroscopy*, 2nd ed.; Springer-Verlag: Berlin, 2003.

(37) Hitchcock, A. P. *aXis*, Version 17-Sep-08, 2008.

Table 1. Crystal Data and Structure Refinement for $La_2U_2Se_9$

fw (g/mol)	1464.52
space group	*Pmma*
Z	2
a (Å)	10.920(2)
b (Å)	5.6100(11)
c (Å)	10.703(2)
V (Å^3)	655.7(2)
T (K)	100(2)
λ (Å)	0.71073
ρ_c (g cm^{-3})	7.418
μ (mm^{-1})	55.938
$R(F)^a$	0.0264
$R_w(F_o^2)^b$	0.0741

$^a R(F) = \sum ||F_o| - |F_c||/\sum |F_o|$ for $F_o^2 > 2\sigma(F_o^2)$. $^b R_w(F_o^2) = \{\sum w(F_o^2 - F_c^2)^2/\sum wF_o^4\}^{1/2}$ for all data. For $F_o^2 < 0$, $w^{-1} = \sigma^2(F_o^2)$; for $F_o^2 \geq 0$, $w^{-1} = \sigma^2(F_o^2) + (0.02 \times F_o^2)^2$.

Table 2. Selected Interatomic Distances (Å) and Angles (deg) for $La_2U_2Se_9$

La(1)−Se(1) × 2	3.0373(9)	Se(3)−Se(3)	2.712(3), 2.748(3)
La(1)−Se(2) × 2	3.333(2)	Se(4)−Se(4)	2.803(3), 2.807(3)
La(1)−Se(4) × 4	3.1642(8)	Se(5)−Se(5)	2.796(3), 2.814(3)
La(1)−Se(5) × 2	3.335(2)	La(1)···U	4.3930(7)
La(2)−Se(2) × 2	3.140(2)	La(2)···U	4.5502(8)
La(2)−Se(3) × 4	3.1364(8)	U···U	5.327(1)
La(2)−Se(5) × 2	3.140(2)		
U−Se(1)	2.8915(8)	Se(1)−Se(1)−Se(1)	180
U−Se(2) × 2	2.9588(7)	Se(2)−Se(2)−Se(2)	180
U−Se(3)	2.976(1)	Se(3)−Se(3)−Se3)	179.90(5)
U−Se(4) × 2	3.0140(9)		
U−Se(5) × 2	3.0361(9)		
U−Se(3)	3.040(1)		

materials for the XANES spectra were synthesized according to literature procedures: β-USe_2,[38] USe_3,[39] and $RbAuUSe_3$.[40]

Results

Synthesis. $La_2U_2Se_9$ was originally obtained from the reaction of U, La, Se, Ba, Sb, and Se at 1123 K in an attempt to produce a quaternary Ba/La/U/Se phase with Sb acting as a flux. Small black metallic blocks of $La_2U_2Se_9$ were produced in approximately 5% yield, based on U. The majority product was an amorphous black melt. A rational synthesis was sought to prepare additional material for physical property measurements. Numerous trials confirmed that the presence of Ba in the reaction mixture was not essential to the formation of $La_2U_2Se_9$. A 2:2:9 stoichiometric ratio of the elements was reacted with various agents ($LaCl_3$, CsCl, I_2, Sb) to induce crystallization, but the yield of product was minimal (< 10%) in each case. Finally, a synthesis utilizing the stoichiometric combination of the elements in a Sb_2Se_3 flux at 1123 K afforded a near quantitative yield of $La_2U_2Se_9$. Sb_2Se_3 had previously been shown to act as an effective flux for the synthesis of some interlanthanide compounds, such as Ln_3LuSe_6 (Ln = La, Ce)[41] and $EuLn_2Se_4$ (Ln = Tb−Lu).[42] A few black prisms of La_2USe_5[10] also formed; this compound is an ordered variant of the U_3S_5 structure type.[8]

(38) Noël, H.; Potel, M.; Troc, R.; Shlyk, L. *J. Solid State Chem.* **1996**, *126*, 22–26.

(39) Kwak, J.-eun; Gray, D. L.; Yun, H.; Ibers, J. A. *Acta Crystallogr., Sect. E: Struct. Rep. Online* **2006**, *62*, i86–i87.

(40) Bugaris, D. E.; Ibers, J. A. *J. Solid State Chem.* **2009**, *182*, 2587–2590.

(41) Jin, G. B.; Choi, E. S.; Guertin, R. P.; Brooks, J. S.; Booth, C. H.; Albrecht-Schmitt, T. E. *Inorg. Chem.* **2007**, *46*, 9213–9220.

(42) Jin, G. B.; Choi, E. S.; Guertin, R. P.; Albrecht-Schmitt, T. E. *J. Solid State Chem.* **2008**, *181*, 14–19.
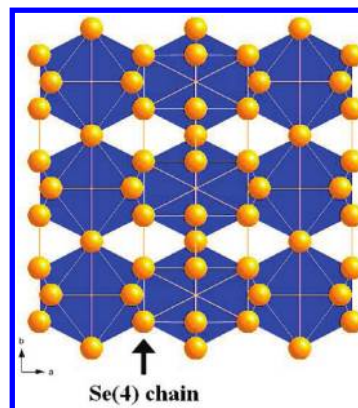
Figure 2. Crystal structure of $La_2U_2Se_9$, viewed down [010].

Figure 3. Uranium selenide layer in $La_2U_2Se_9$, featuring the infinite Se(5) polyselenide chain, as viewed along [001].

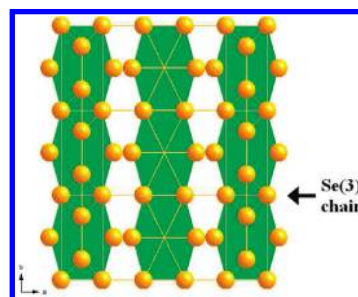**Figure 4.** La(1) selenide layer in $La_2U_2Se_9$, featuring the infinite Se(4) polyselenide chain, as viewed along [001].

**Figure 5.** La(2) selenide layer in $La_2U_2Se_9$, featuring the infinite Se(3) polyselenide chain, as viewed along [001].

Structure. $La_2U_2Se_9$ crystallizes in a new structure type (Figure 2) in space group *Pmma* of the orthorhombic system. The asymmetric unit of $La_2U_2Se_9$ contains the following atoms (and their site symmetries): U (*.m.*); La(1) (*mm2*); La(2) (*mm2*); Se(1) (*mm2*); Se(2) (*.m.*); Se(3) (*.m.*); Se(4) (*.2.*); and Se(5) (*m..*). Atom U is coordinated by nine Se atoms in a monocapped square antiprism; atom La(1) is coordinated by 10 Se atoms in a geometry most closely resembling a bicapped square prism; and atom La(2) is coordinated by eight Se atoms in a bicapped trigonal prism.

The complex three-dimensional structure of $La_2U_2Se_9$ consists of alternating U/Se and La/Se layers that stack in the [001] direction. Within the U/Se layer (Figure 3), each USe_9 unit shares an edge and a corner with neighboring USe_9 units in the [100] direction, and shares two corners in the [010] direction. The Se(5) atoms form infinite linear chains in the [010] direction. In these chains the Se−Se distances alternate between 2.796(3) and 2.814(3) Å. The shorter Se−Se distances in the chains constitute the shared edges between USe_9 units within a layer.

The next layer in the [001] direction contains only $La(1)Se_{10}$ bicapped square prisms that point successively up or down as one proceeds along the [100] direction. Each $La(1)Se_{10}$ unit shares edges with its neighbors in the [100] direction, and shares two corners in the [010] direction (Figure 4). The Se(4) atoms form infinite linear chains in the [010] direction. In these chains the Se−Se distances alternate between 2.803(3) and 2.807(3) Å. The statistically insignificantly longer Se−Se distances of the chains form the edges shared between adjacent $La(1)Se_{10}$ units.

Continuing in the [001] direction one finds another U/Se layer, identical to the first, followed by a layer containing only $La(2)Se_8$ bicapped trigonal prisms. These $La(2)Se_8$ polyhedra point successively up or down along the [100] direction. Each $La(2)Se_8$ unit shares edges with neighboring $La(2)Se_8$ units in the [010] direction (Figure 5). The Se(3) atoms form a third polyselenide chain, this time extending in the [100] direction, with distances alternating between 2.712(3) and 2.748(3) Å. The Se−Se−Se angle is 179.90(5)°. The longer Se−Se distances of the chain constitute the edges shared between adjacent $La(2)Se_8$ units.

The layers of $La_2U_2Se_9$ stack in the sequence *USe La(1)Se USe La(2)Se USe* as a consequence of bonding between layers (Figure 6). A given USe_9 unit shares two edges and two faces with the $La(1)Se_{10}$ units above it, as well as an edge with the next USe_9 unit. The same USe_9 unit also shares four edges with $La(2)Se_8$ units below it, as well as an edge with the subsequent USe_9 unit. The shorter Se−Se distances of the Se(3) and Se(4) polyselenide chains form the shared edges between USe_9 units stacked in the [001] direction. A given $La(1)Se_{10}$ unit shares four edges and four faces with the closest USe_9 units, as well as two edges with more distant $La(2)Se_8$ units. The longer Se−Se distances of the Se(5) polyselenide chain constitute one of the sets of edges shared between $La(1)Se_{10}$ and $La(2)Se_8$ units stacked in the [001] direction. Each $La(2)Se_8$ unit shares eight edges with the nearest USe_9 units, as well as two edges with further $La(1)Se_{10}$ units.

Magnetic Susceptibility Measurement. The inverse magnetic susceptibility of $La_2U_2Se_9$ for both ZFC and FC data, as a function of temperature, is shown in Figure 7. The magnetic susceptibility of $La_2U_2Se_9$ shows
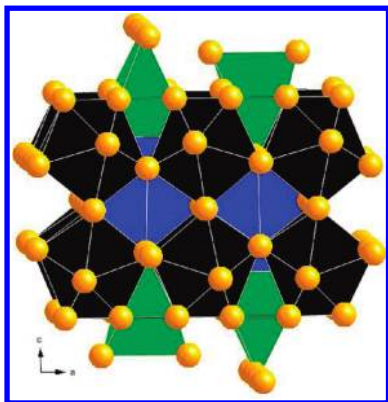
Figure 6. Polyhedral representation of the three-dimensional, multilayered structure of $La_2U_2Se_9$, as viewed down [010].
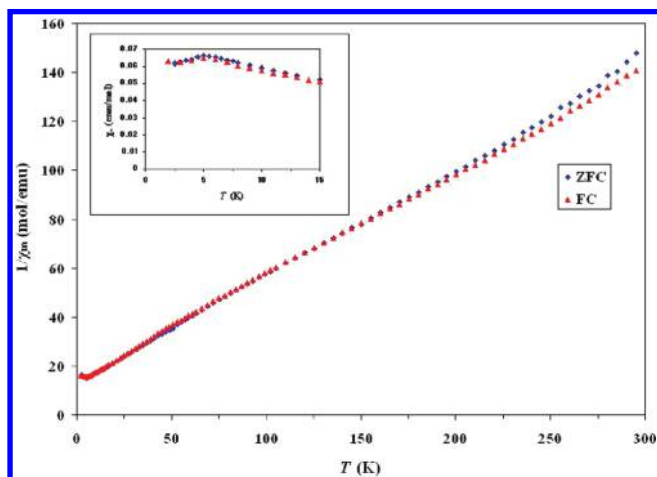
Figure 7. Inverse magnetic susceptibility ($1/\chi_m$) vs T for $La_2U_2Se_9$. (Inset: The low temperature magnetic susceptibility (χ_m) vs T for $La_2U_2Se_9$, showing $T_N = 5$ K).

a maximum at $T_N = 5$ K (see inset in Figure 7), indicative of an antiferromagnetic transition. A number of ternary transition metal uranium selenides, including MU_8Se_{17} (M = Ti−Ni),[43] $M_2U_6Se_{15.5}$ (M = Rh, Ir),[44] and Cu_2U_3-Se_7,[45]exhibit antiferromagnetic transitions. The Néel temperatures range from a low of 5.5 K in TiU_8Se_{17} to a high of 75 K in $Ir_2U_6Se_{15.5}$.

For $La_2U_2Se_9$, the inverse magnetic susceptibility data vary linearly with temperature above 50 K and can be fit to the Curie−Weiss law $\chi^{-1} = (T - \theta_p)/C$. The values of the Curie constant C and the Weiss constant θ_p are 2.409(9) emu K mol^{-1} and $-38.5(7)$ K, respectively. The large negative value of θ_p for $La_2U_2Se_9$ is consistent with the antiferromagnetic ordering, as observed in other transition-metal uranium selenides, such as TiU_8Se_{17} ($T_N = 5.5$ K, $\theta_p = -40$ K) and VU_8Se_{17} ($T_N = 31$ K, $\theta_p = -70$ K),[43] and $Cu_2U_3Se_7$ ($T_N = 13$ K, $\theta_p = -28$ K).[45] The effective magnetic moment, μ_{eff}, as calculated from the equation $\mu_{eff} = (7.997C)^{1/2} \mu_B$,[46] is 3.10(1) μ_B/U. This effective magnetic moment can be compared to the values of the free-ion moments for U^{3+} (3.62 μ_B),
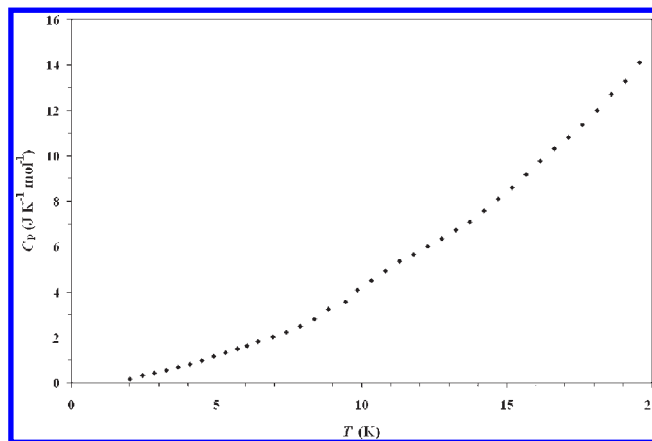
Figure 8. Specific heat (C_p) vs T for $La_2U_2Se_9$.

U^{4+} (3.58 μ_B), and U^{5+} (2.54 μ_B), calculated from L-S coupling.[47] No magnetic measurements exist for U(III) or U(V) selenides, but the value of μ_{eff} of 3.10(1) μ_B/U for $La_2U_2Se_9$ is within the range of measured values for other U(IV) selenides, including 3.0 μ_B/U for VU_8Se_{17},[43] 3.2 μ_B/U for MgU_8Se_{17},[43] 3.27 μ_B/U for $Cu_2U_6Se_{13}$,[48] and 3.3 μ_B/U for CoU_8Se_{17}.[43] The fact that the observed effective magnetic moments for these compounds are lower than the theoretical free-ion moment for U(IV) has been attributed to crystal-field effects.[45]

Specific Heat Measurement. The temperature dependence of the specific heat, C_p, was collected between 1.8 and 20 K with no applied field (Figure 8). There is neither long-range ordering nor a phase transition at or around 5 K (T_N). The specific heat is of the form $C_p = \gamma T + \beta T^3$, where γ is the electronic contribution and β is the lattice contribution. For the temperature range 10 K $< T <$ 20 K, the data can be fit to afford the values $\gamma = 336(3)$ mJ K^{-2} mol^{-1} and $\beta = 1.00(1)$ mJ K^{-4} mol^{-1}. The Debye temperature, Θ_D, can be estimated from the equation $\beta = (12\pi^4 nR)/(5\Theta_D{}^3)$, where R is the gas constant and n is the number of atoms per formula unit.[49] A value of 293(1) K is found for Θ_D. A comparison with literature values is complicated by the fact that very few specific heat measurements have been performed on uranium chalcogenides, and, to the best of our knowledge, none on ternary chalcogenide compounds. Some values of γ, β, and Θ_D for binary uranium chalcogenides are summarized in Table 3. The values of β and Θ_D for $La_2U_2Se_9$ are consistent with those values determined for the binary uranium chalcogenides. Conversely, the value of γ is significantly larger for $La_2U_2Se_9$ than for any of the binary uranium chalcogenides. Yet, it is too small to be indicative of heavy fermion behavior where γ is typically larger than 1 J K^{-2} mol^{-1}.[49] Some uranium intermetallics, including UBe_{13}[50] and UPt_3,[51] are heavy fermion materials.

(43) Noël, H.; Troc, R. *J. Solid State Chem.* **1979**, *27*, 123–135.
(44) Daoudi, A.; Noël, H. *J. Alloys Compd.* **1996**, *233*, 169–173.
(45) Daoudi, A.; Lamire, M.; Levet, J. C.; Noël, H. *J. Solid State Chem.* **1996**, *123*, 331–336.
(46) O'Connor, C. J. *Prog. Inorg. Chem.* **1982**, *29*, 203–283.

(47) Kittel, C. *Introduction to Solid State Physics*, 7th ed.; Wiley: New York, 1996.
(48) Noël, H. *J. Less-Common Met.* **1980**, *72*, 45–49.
(49) *The Specific Heat of Matter at Low Temperatures*; Tari, A., Ed.; Imperial College Press: London, 2003.
(50) Ott, H. R.; Rudigier, H.; Fisk, Z.; Smith, J. L. *Phys. Rev. Lett.* **1983**, *50*, 1595–1598.
(51) Stewart, G. R.; Fisk, Z.; Willis, J. O.; Smith, J. L. *Phys. Rev. Lett.* **1984**, *52*, 679–682.

Table 3. Heat Capacity Data for Selected Uranium Chalcogenides

compound	T (K)	γ (mJ K^{-2} mol^{-1})	β (mJ K^{-4} mol^{-1})	Θ_D (K)	reference
La$_2$U$_2$Se$_9$	$1.8 < T < 20$	336(3)	1.00(1)	293(1)	this work
US	$1.25 < T < 4.55$	25.3	0.330	181	77
U$_2$S$_3$	$160 < T < 300$	44(3)	0.304(9)^a	$3.2(1) \times 10^2$	78
USe	$0.12 < T < 12$	14.7(6)	0.763(9)^a	172(2)	79
U$_2$Se$_3$	$160 < T < 300$	99(8)	1.0(1)^a	$2.1(2) \times 10^2$	78
UTe	$0.12 < T < 12$	10.3(4)	2.03(3)^a	124(2)	79

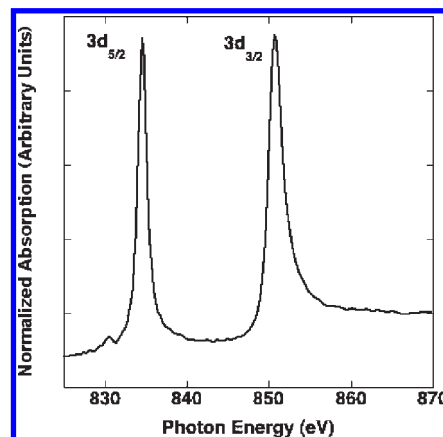^{a} Calculated from the equation $\beta = (12\pi^4 nR)/(5\Theta_D{}^3)$.
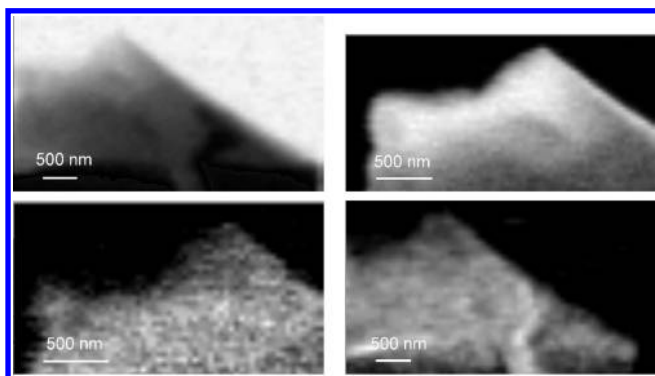
Figure 9. Four images of the particle obtained from powdered La$_2$U$_2$Se$_9$, from which XANES spectra were collected: normal contrast image obtained with a photon energy of 1415.0 eV (upper left); an elemental map of La obtained by subtraction using photon energies of 828.0 and 834.6 eV with the regions containing La shown as white using a standard gray scale (upper right); an elemental map of U obtained by subtraction using photon energies of 728.0 and 737.0 eV with the regions containing U shown as white (lower left); and an elemental map of Se obtained with photon energies of 1425.0 and 1452.0 eV with regions containing Se shown as white (lower right).

Figure 10. Lanthanum 3d$_{5/2,3/2}$ absorption spectrum as collected from La$_2$U$_2$Se$_9$.

Scanning Transmission X-ray Microscopy (STXM) Spectromicroscopy. Figure 9 shows a normal contrast image as well as the respective elemental constituent maps of the La$_2$U$_2$Se$_9$ particle from which XANES spectra were recorded. The X-ray images show that the particle is uniform in composition at the nanometer scale. No sample degradation was observed during the period of the data collection.

Lanthanum XANES. The La 3d-edge XANES spectrum from La$_2$U$_2$Se$_9$ as collected (normalized to the photon flux) is shown in Figure 10 with the atomic-like La 3d$_{5/2,3/2}$ white line transitions being the most noticeable features appearing at 834.6 and 851.0 eV, respectively. The La spectrum is characteristic of a trivalent species, including the small feature at 830.4 eV, as judged by comparison to previous results that exhibit these features at these energies with the same spin−orbit splitting of 16.2 eV.[52,53]

Uranium XANES. The U 4d-edge XANES spectrum from La$_2$U$_2$Se$_9$ is shown in Figure 11 along with those from β-USe$_2$ and RbAuUSe$_3$. The latter have had backgrounds subtracted whereas that from La$_2$U$_2$Se$_9$ has not. All spectra have been 3-point smoothed and normalized to the U 4d$_{5/2}$ feature. The distinct U 4d$_{5/2}$ and U 4d$_{3/2}$

transitions are the most prominent features of these spectra. The broad feature between white lines has been observed previously in U spectra. It is independent of the oxidation state of U, but it has yet to be assigned. However, the broad feature in the RbAuUSe$_3$ spectrum beginning just after 760 eV and tailing into the U 4d$_{3/2}$ features is absorption from the Au constituent at ∼ 763 eV (Au 4s). These transitions from the U 4d orbitals primarily probe unoccupied states with U 5f character. The charge-state shift of the U 4d$_{5/2}$ transition can be used to assign an effective oxidation state based on the energy of the U 4d$_{5/2}$ transition. When coupled with the 4d$_{3/2}$ transition, it can provide additional information on bonding characteristics.[54−56]

The U 4d$_{5/2}$ and U 4d$_{3/2}$ transitions for La$_2$U$_2$Se$_9$ are found at 736.9 and 778.3 eV, respectively. These compare well to the corresponding U 4d-edges energies obtained from a well-characterized U^{4+} reference material, RbAuUSe$_3$, at 736.9 and 778.1 eV. Furthermore, the spectrum of another similar U^{4+} selenide, β-USe$_2$, has 4d-edges at 736.6 and 777.8 eV. Although not shown in Figure 11, USe$_3$ has a U 4d$_{5/2}$ transition at 736.9 eV. Other common U^{4+} solid-state materials such as UCl$_4$ and UO$_2$ have 4d$_{5/2}$ transitions at 737.1 and 738.5 eV, respectively, whereas the U^{4+} complex with 2,6-bis-(2-benzimidazyl)pyridine (BBP), [U(BBP)$_3$]Cl$_4$, has U 4d-edge transitions at 736.9 and 778.4 eV. The U materials in this study have 4d$_{5/2}$ transitions that lie above the

(52) Thole, B. T.; van der Laan, G.; Fuggle, J. C.; Sawatzky, G. A.; Karnatak, R. C.; Esteva, J.-M. *Phys. Rev. B: Condens. Matter* **1985**, *32*, 5107–5118.

(53) Shuh, D. K.; Terminello, L. J.; Boatner, L. A.; Abraham, M. M. *Mater. Res. Soc. Symp. Proc.* **1993**, *307*, 95–100.

(54) Nilsson, H. J.; Tyliszczak, T.; Wilson, R. E.; Werme, L.; Shuh, D. K. *Anal. Bioanal. Chem.* **2005**, *383*, 41–47.

(55) Nilsson, H. J.; Tyliszczak, T.; Wilson, R. E.; Werme, L.; Shuh, D. K. In *Recent Advances in Actinide Science*; May, I., Bryan, N. D., Alvares, R., Eds.; Royal Society of Chemistry: London, 2006; pp 56−58.

(56) Moore, K. T.; van der Laan, G. *Rev. Mod. Phys.* **2009**, *81*, 235–298.
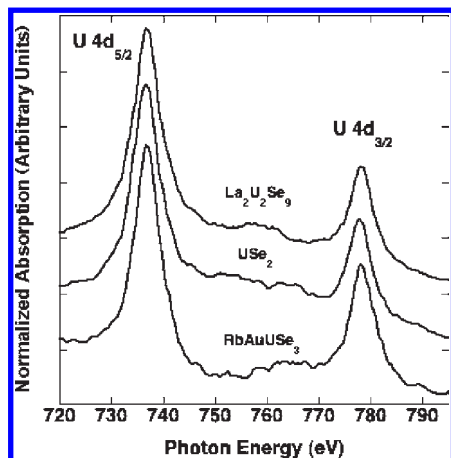
Figure 11. Uranium $4d_{5/2,3/2}$ absorption spectrum as collected from $La_2U_2Se_9$ (top), β-USe_2 (middle), and $RbAuSe_3$ (bottom).

transition energy of 736.6 eV that has been determined for a well-characterized U^{3+} complex, $[U(BBP)_3]I_3$.[34,57] Recently, the $4d_{5/2}$-edge position for another U^{3+} complex, $(CpSiMe_3)_3UAlCp^*$, was found at 736.7 eV.[35] The lower energy charge-state boundary is set by U metal with a U $4d_{5/2}$ transition at 736.4 eV.[58]

The branching ratio ($4d_{5/2}$:$4d_{3/2}$) derived from the peak intensities of $La_2U_2Se_9$ is similar to those observed from β-USe_2, the BBP complexes, and $RbAuSe_3$ (part of the $4d_{3/2}$ feature is augmented from Au 4s absorption). The energy position of the U $4d_{5/2}$ transition of $La_2U_2Se_9$ is above the energies observed for metallic U and nearly all U^{3+} complexes, and within the range established for similar U^{4+} materials. Thus, the charge-state shift of $La_2U_2Se_9$ corresponds to a U^{4+} species. Note that the U $4d_{5/2}$ charge-state shift of β-USe_2 is on the boundary of the U^{4+}-U^{3+} charge states.

Selenium XANES. The Se $2p_{3/2,1/2}$ near-edge spectra recorded from USe_3, $La_2U_2Se_9$, β-USe_2, $RbAuSe_3$, and elemental Se are shown in Figure 12. Backgrounds were subtracted from these Se XANES spectra; they were then 5-point smoothed and normalized to the signal at 1520 eV. The $2p_{3/2,1/2}$ transitions indicated in Figure 12 occur at about 1433.9 and 1474.3 eV. XANES spectroscopy of the Se 2p-edge has not been employed extensively to determined oxidation states of Se materials; however, there have been some investigations.[59,60] The $RbAuSe_3$ and β-USe_2 spectra provide well-characterized reference materials known to contain only discrete Se^{2-} anions. Because USe_3 can be represented formally as (U^{4+})-$(Se^{2-})(Se_2^{2-})$,[61] its spectrum should display both Se^{2-} and Se_2^{2-} components.
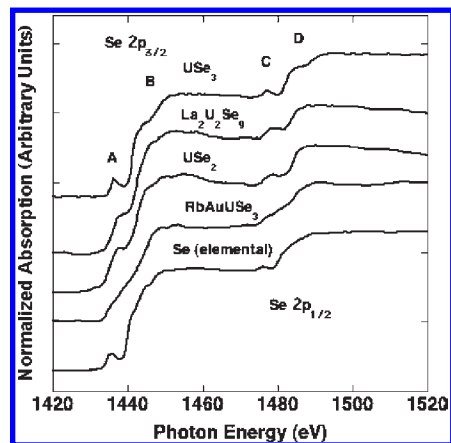
Figure 12. Selenium $2p_{3/2,1/2}$ absorption spectrum obtained from USe_3, $La_2U_2Se_9$, β-USe_2, $RbAuSe_3$, and elemental Se (top to bottom).

The Se L-edge XANES spectrum of $La_2U_2Se_9$ shown in Figure 12 has distinguishable features centered at about 1438.1 eV (A), a broad feature extending between $\sim$1440$-$1460 eV (B), a distinct peak at 1478.9 eV (C), and a final broad feature appearing at 1481.3$-$1500 eV (D). The β-USe_2 Se 2p spectrum is nearly identical to that of $La_2U_2Se_9$. The XANES spectrum of $RbAuSe_3$ has a very small feature at 1436.6 eV, a broad, smooth feature from about 1440$-$1460 eV, no feature in location (C), and a final broad feature starting at 1473.9 eV extending out to 1500 eV. The reference for mixed Se speciation, USe_3, has features at 1437.7 eV, a broad feature present from 1439.2 to 1461.5 eV, a notable peak at 1478.5 eV, and a broad feature from 1481.3 to 1500 eV.

The Se 2p spectrum from the $La_2U_2Se_9$ is nearly the same as the spectra obtained from β-USe_2 and $RbAu$-USe_3. However, the $La_2U_2Se_9$ spectrum does not exhibit the prominent feature at (A) and has differences in line shape near (B) when compared to the spectrum from USe_3. Thus, the Se 2p spectra provide support for the presence of discrete Se^{2-} units in $La_2U_2Se_9$ but do not provide evidence for the existence of Se_2^{2-}.

Formal Oxidation States

The complex structure of $La_2U_2Se_9$ complicates the assignment of formal oxidation states to the elements. La is unequivocally $+III$, as supported by both XANES and the normal La$-$Se distances. These La$-$Se distances are 3.0373(9) to 3.335(2) Å, versus 2.9830(7) to 3.2235(7) Å in $LaCuSe_2$,[62] and 2.960(1) to 3.377(1) Å in $LaYbSe_3$.[63]

The Se atoms in $La_2U_2Se_9$ have the following interactions: Se(1): U and La(1); Se(2): U and La(2); Se(3): La(1) and Se(3); Se(4): La(2) and Se(4); Se(5): U and Se(5). Atoms Se(1) and Se(2), having interactions only with the metals, are discrete Se^{2-} anions, which can be seen in the Se XANES spectrum. Assignment of formal oxidation states to atoms Se(3), Se(4), and Se(5) is problematic, given that each takes part in a linear infinite chain with Se$-$Se distances ranging from 2.712(3) to 2.814(3) Å. These distances are significantly longer than that of an average Se$-$Se single bond in α-Se_8

(57) Copping, R.; Teat, S. J.; Janousch, M.; Tyliszczak, T.; Shuh, D. K., in preparation (**2010**).

(58) Center for X-ray Optics, X-ray Interactions with Matter; LBNL: Berkeley, CA, U.S.A.; http://www.cxro.lbl.gov/optical-constants.

(59) Wolska, A.; Bacewicz, R.; Filipowicz, J.; Attenkofer, K. *J. Phys.: Condens. Matter* **2001**, *13*, 4457–4470.

(60) Madwid, J.; Andrahennadi, R.;. Blyth, R.; Coulthard, I.; Doonan, C. J.; Liu, D.; Hoffmeyer, R.; Pushie, M. J.; Regier, T.; Ruszkowski, J.; Singh, S. P.; Thavarajah, D.; Wiramanaden, C. I. E. Yang, S. I. ; Zhang, L.; George, G. N.;. Pickering, I. J. *Earth and Environment Science Report*; Canadian Light Source, Inc.: Saskatoon, Saskatchewan, Canada, 2004.

(61) Ben Salem, A.; Meerschaut, A.; Rouxel, J. *C. R. Acad. Sci., Sér. 2* **1984**, *299*, 617–619.

(62) Ijjaali, I.; Mitchell, K.; Ibers, J. A. *J. Solid State Chem.* **2004**, *177*, 760–764.

(63) Mitchell, K.; Somers, R. C.; Huang, F. Q.; Ibers, J. A. *J. Solid State Chem.* **2004**, *177*, 709–713.

(2.30(2) Å)[64] or in USe₃ (2.361(2) Å),[61] but much shorter than the sum of the van der Waals radii of two Se atoms (3.64 Å).[29] Some other known compounds exhibit longer than expected Se—Se bond distances, including Nb_2Se_9 (2.663(2) Å),[65] $K_3CuNb_2Se_{12}$ (2.726(3) Å),[66] $Rb_{12}Nb_2Se_{35}$ (2.644(2) Å),[67] $K_{12}Ta_2Se_{35}$ (2.6409(12) Å),[68] and $Cs_4Th_4P_4Se_{26}$ (2.645(2) Å).[69] However, none of these compounds contains an infinite polyselenide chain as does $La_2U_2Se_9$. Their unusual Se coordination environments have been assigned, in some cases rather arbitrarily, as follows: Nb_2Se_9 has an Se_5^{4-} anion, $K_3CuNb_2Se_{12}$ has a Se_4^{2-} anion, $Rb_{12}Nb_2Se_{35}$ and $K_{12}Ta_2Se_{35}$ each have an Se_4^{3-} anion, and $Cs_4Th_4P_4Se_{26}$ has a near linear Se_3 fragment in a $P_2Se_9^{4-}$ anion.

From the Se XANES spectrum of $La_2U_2Se_9$ we cannot assign oxidation states to the Se(3), Se(4), and Se(5) atoms. Given our inability to assign formal oxidation states to all of the Se atoms in $La_2U_2Se_9$, we cannot assign an oxidation state to the U atom by charge balance. Formal oxidation states for U of +III, +IV, +V, and +VI are found in solid-state compounds, with the +IV oxidation state favored in chalcogenides. Let us consider these possibilities in turn. Given that $La_2U_2Se_9$ is magnetic and that a compound of La(III) and U(VI) would be diamagnetic, the +VI oxidation state for U is not possible. The μ_{eff} value of 3.10(1) μ_B/U for $La_2U_2Se_9$ is not indicative of U(V), but does correspond with the measured values for other U(IV) selenides in the literature. However, it has been noted[70] that magnetic measurements are not a generally reliable way to distinguish among formal oxidation states for U.

It is difficult to assign the oxidation state of U as +III, +IV, or +V, solely on the basis of bond distances. For a comparison of bond distances to have merit, the bonding environment (ligand type and coordination number) must be identical. The only possible U^{5+} selenide compound in the literature, whose structure is based on single-crystal X-ray diffraction data, is UAsSe,[71] with U—Se bond distances of 2.934(1) to 3.030(8) Å. However, the bonding environment around U in this compound involves five Se anions and four As anions. Moreover, there is some ambiguity as to whether the oxidation states in UAsSe are U^{5+}, As^{3-}, and Se^{2-}, or U^{4+}, As^{2-}, and Se^{2-}. The only possible U^{3+} selenide in the literature is U_2Se_3,[72] which was determined from powder X-ray diffraction data to be isostructural with Sb_2S_3. Once again, the bonding environment around U in this compound is different from that in $La_2U_2Se_9$, because the coordination number of U is only seven rather than nine. Nevertheless, the U—Se bond distances are 2.723(1) to 3.043(1) Å in U_2Se_3. An indirect argument against the presence of U^{3+} in $La_2U_2Se_9$ is that the compound is ordered. The difference in ionic radii between U^{4+} in six coordination and nine coordination is 0.16 Å. If we apply this difference to the ionic radius for U^{3+} in six coordination of

1.165 Å, we expect the ionic radius of U^{3+} in nine coordination to be 1.325 Å. The ionic radii of La^{3+} in eight coordination and ten coordination are 1.300 Å and 1.41 Å, respectively. Thus, disorder of U^{3+} and La^{3+} over the same site or sites would be expected. However, the significantly smaller ionic radius of U^{4+} (1.19 Å)[29] in nine coordination would most likely cause La^{3+} and U^{4+} to occupy unique crystallographic sites.

There are numerous examples of U^{4+} selenides in the literature, but only three in which the coordination number of U is nine. These examples of nine-coordinate U^{4+} selenides, along with their U—Se bond distances, are as follows: β-USe₂ (2.850(4)—3.250(3) Å),[38] γ-USe₂ (2.818(6)—3.123(4) Å),[73] and $K_2UP_3Se_9$ (2.914(3)—3.273(3) Å).[74] These U—Se bond distances compare favorably with those of 2.8915(8) to 3.040(1) Å in the present $La_2U_2Se_9$. As noted above, the formal oxidation state of +IV for U in $La_2U_2Se_9$ is confirmed by the U XANES spectrum.

Bond valence analysis[75] provides another means of assigning formal oxidation states. Because it is based on data from bond distances we would expect it to provide results consistent with the arguments above. Indeed it does, as the Bond Valence function in PLATON[76] leads to the following oxidation states for $La_2U_2Se_9$: U 4.13; La(1) 2.97; La(2) 2.72.

From the sum of these arguments (bond distances, bond valence analysis, magnetic susceptibility, and XANES), we believe that $La_2U_2Se_9$ is a compound of La(III) and U(IV). It is interesting that on the basis of charge balance such an assignment leaves a total charge of −4 to be distributed among atoms Se(3), Se(4), and Se(5).

Supporting Information Available: The crystallographic file in CIF format for $La_2U_2Se_9$, as well as additional experimental details for the Scanning Transmission X-ray Microscopy (STXM) Spectromicroscopy. This material is available free of charge via the Internet at http://pubs.acs.org.

(64) Maaninen, A.; Konu, J.; Laitinen, R. S.; Chivers, T.; Schatte, G.; Pietikäinen, J.; Ahlgrén, M. *Inorg. Chem.* **2001**, *40*, 3539–3543.
(65) Sunshine, S. A.; Ibers, J. A. *Acta Crystallogr., Sect. C: Cryst. Struct. Commun.* **1987**, *43*, 1019–1022.
(66) Lu, Y.-J.; Ibers, J. A. *Inorg. Chem.* **1991**, *30*, 3317–3320.
(67) Dürichen, P.; Bolte, M.; Bensch, W. *J. Solid State Chem.* **1998**, *140*, 97–102.
(68) Tougait, O.; Ibers, J. A. *Solid State Sci.* **1999**, *1*, 523–534.
(69) Briggs Piccoli, P. M.; Abney, K. D.; Schoonover, J. D.; Dorhout, P. K. *Inorg. Chem.* **2001**, *40*, 4871–4875.
(70) Tougait, O.; Potel, M.; Noël, H. *J. Solid State Chem.* **2002**, *168*, 217–223.
(71) Pietraszko, D.; Lukaszewicz, K. *Bull. Acad. Pol. Sci., Ser. Sci. Chim.* **1975**, *23*, 337–340.
(72) Khodadad, P. *C. R. Hebd. Seances Acad. Sci.* **1959**, *249*, 694–696.

(73) Kohlmann, H.; Beck, H. P. *Z. Anorg. Allg. Chem.* **1997**, *623*, 785–790.
(74) Chondroudis, K.; Kanatzidis, M. G. *C. R. Acad. Sci. Paris* **1996**, *322*, 887–894.
(75) Brown, I. D. *The Chemical Bond in Inorganic Chemistry, The Bond Valence Model*; Oxford University Press: New York, 2002.
(76) Spek, A. L. *PLATON, A Multipurpose Crystallographic Tool*, 2008.
(77) Gordon, J. E.; Troc, R. *Phys. Rev. B: Condens. Matter* **1986**, *33*, 578–580.
(78) Lagnier, R.; Wojakowski, A.; Suski, W.; Janus, B.; Mortimer, M. J. *Phys. Status Solidi A* **1980**, *57*, K127–K132.
(79) Rudigier, H.; Ott, H. R.; Vogt, O. *Phys. Rev. B: Condens. Matter* **1985**, *32*, 4584–4591.